

Estimation of pulse shaping for well-logs

K. Sølna*

February 26, 1999

Abstract

A wavelet propagating in a finely layered lossless medium is subject to apparent attenuation that changes its shape. Can a sonic log be used to characterize this change? We show that numerical simulations with the well-log as medium give an apparent attenuation or diffusion of the pulse which is very different from the attenuation in the real medium, this is due to the smoothing effect of the well-log tool. Based on a version of the O’Doherty-Anstey approximation we derive an expression that reveals the role of the tool. Using a sonic log we verify the theory and show how tool effects can be mitigated by deconvolution. We also propose a two-scale stochastic model for the sonic log and a procedure for estimation of its parameters. One application of sonic logs is exactly to quantify apparent attenuation and in this context our results are important.

1 Introduction

The earth comprises heterogeneities on many scales and a wavelet traveling through the heterogeneous earth is transformed due to scattering associated with *fine* scale fluctuations in the medium parameters. We refer to this phenomenon as apparent attenuation. Synthetic seismograms can be used in order to describe such effects for a particular geology. Here we want to examine the consequence of using a seismic well-log as a model for a layered medium in wave simulations. A second objective is to derive a framework for estimation of the microscale parameters of the medium.

The analysis is based on a generalization of the O’Doherty-Anstey approximation. This approximation characterizes the transformation of the pulse shape based on a stochastic model for the medium. The well-log tool alters the statistics of the fluctuations in the medium and the O’Doherty-Anstey approximation reveals how this affects apparent attenuation. We illustrate with computations based on a well-log from the North Sea and obtain excellent agreement with the theory. Models for both the medium and the well-log tool are used in the analysis. For the tool we use a model similar to that used in [7]. For the medium we introduce a two-scale stochastic model and discuss estimation of its parameters. An important aspect of the estimation procedure is that it takes the tool into account.

Realizing the importance of the approximation presented by O’Doherty and Anstey [11] a number of authors have reexamined it and extended it to more general wave propagation scenarios [1, 3, 4, 6, 8, 9, 12, 13, 17]. Here we consider acoustic wave propagation in a layered medium with *weak* fluctuations. Based on the analysis in [8, 17], we obtain an approximation that reveals how the tool affects the propagating wave. Note that apparent attenuation becomes important only for relatively long propagation distances. As pointed out in [3], the O’Doherty-Anstey approximation goes somewhat beyond averaging as in [2] in that it deals with such long propagation distances.

*Department of Mathematics, University of Utah, Salt Lake City, Utah 84112; solna@math.utah.edu

That apparent attenuation effects are important in the seismic wave propagation context has been shown for instance in [14, 15]. Marion et al. [10] present a study that also demonstrates the importance of medium fluctuations at different scales. They affect the travel time and dispersion of the wavelet. The authors explore approximations that characterize these effects. To apply these however, one needs reliable information about the medium fluctuations. We show that information about the fine scales are strongly corrupted by the tool and that this can lead to erroneous results unless compensated for.

The outline of the paper is as follows. In Section 2 we discuss the models for the medium and the tool. Next, in Section 3, we introduce the appropriate version of the O’Doherty-Anstey approximation and discuss the role of the tool. Finally, we illustrate using numerical simulations based on the North Sea log in Section 4.

2 Modeling and estimation

We consider acoustic wave propagation through a layered medium defined by

$$\begin{aligned} \rho(z) &\equiv \rho_0 \\ V(z) &= \begin{cases} V_0 & \text{for } z \leq 0 \\ V_k & \text{for } k\Delta z \leq z \leq (k+1)\Delta z \quad 0 \leq k \leq N \\ V_N & \text{for } N\Delta z \leq z, \end{cases} \end{aligned} \tag{2.1}$$

where z is depth coordinate, $\Delta z = .125m$, ρ is the (constant) density and V the local speed of sound. The V_k ’s are the velocities in the discrete sections. The medium is modeled as *random* and V_k as a stochastic process. We denote by \tilde{V}_k the sonic log from the medium V_k . A plane-wave impulse is impinging upon the medium at the surface $z = 0$. We are interested in its shape when it has propagated to depth $L = N\Delta z$, either in the medium V_k or in \tilde{V}_k , the medium defined by the log.

Apparent attenuation is caused by the (fine scale) medium variations. We use the following model random medium for these fluctuations

$$V_k = \bar{V}_k(1 + \epsilon e_k \exp(sX_k)). \tag{2.2}$$

Here, \bar{V}_k is a ‘background’ medium modulation that varies on a macroscale, the scale corresponding to L . The random fluctuations are defined by the stationary stochastic process X_k and these fluctuations define the microscale in our modeling. Note that the width of the propagating wavelet is on this scale. The sequence X_k is taken to be a zero-mean unit variance Gaussian sequence. The strength of the fluctuations are $\propto \epsilon e_k$ with e_k varying on the macroscale and $\epsilon \ll 1$. The positive sequence e_k is scaled to unity in root mean square. Thus, we assume that the fluctuations are *weak*, that is the small contrast case. The parameter s is a skewness parameter and the correlations of X_k are

$$E[X_k X_{k+n}] = \exp(-n/l). \tag{2.3}$$

We examine apparent attenuation in V_k and also in the medium defined by the log, \tilde{V}_k , and look at how the attenuation *differ* for these media. The log is related to V_k by the model for the tool

$$\frac{1}{\bar{V}_k} = \sum_{i=1}^M \frac{w_i}{V_{k+i}}, \quad (2.4)$$

with the weights w_i adding to unity [7]. The parameters, w_i and M , are modeled as being independent of the recording location, with M corresponding to the physical length of the tool. Note that the variations in \bar{V}_k are slow relative to M , but that the fine scale fluctuations vary rapidly relative to M .

In order to obtain realistic parameter values for the medium model (2.2) we estimate these using a sonic log from the the Troll-field in the North Sea. This well-log and its estimation is discussed in Appendix A. The moment estimators we present there are based on interface reflections coefficients rather than the velocity observations themselves. The reflections are less sensitive to variations in the macroscale parameters and give more robust estimates for the microscale medium parameters. A second key aspect of the estimation is that the model for the tool is explicitly used. The resulting parameter estimates are $\epsilon = .03$, $s = 1.1$ & $l = 2$. The small value of l implies that the micro-scale fluctuations occur on a very fine scale: $\approx 0.5m$.

3 Apparent attenuation and tool effects

In this section we use O’Doherty-Anstey theory to characterize the shape of the transmitted pulse, the shape at depth $L = N\Delta z$ after the pulse has traveled through the *discrete* medium. The medium is statistically stationary. In the model (2.2) this entails that the macroscale parameters \bar{V}_k & e_k are constant. Note that only their mean square values are important for the apparent attenuation phenomenon.

Denote the (discrete) pulse at the surface $z = 0$ for \mathbf{u}_0 , the pulse is sampled (in time) at rate $\Delta\tau = 2\Delta z/\bar{V}_0$. Then the transmitted *pulse shape* at $z = L$ can be characterized by

$$\mathbf{u}_L \sim \mathbf{u}_0 \star \mathbf{H}_L \quad \text{as } \epsilon \downarrow 0. \quad (3.1)$$

In absence of microscale medium fluctuations the sequence $\mathbf{H}_L = \{H_L(i)\}$ is given by $H_L(0) = 1$ and $H_L(i) = 0$ for $i \neq 0$. Recall that ϵ represents the magnitude of the medium fluctuations and is assumed to be small. We derive (3.1) in Appendix B, where we also discuss the continuous case. The function \mathbf{H}_L is *deterministic*, hence the transformation of the pulse shape due to the random layering is to leading order a deterministic phenomenon. Note, however, that the travel time to depth L contains a small random component, see for instance [17]. The vector \mathbf{H}_L is a causal ‘pulse shaping filter’ and is determined by the medium statistics as we explain next. Let

$$\begin{aligned} \gamma_n &= \frac{E[(V_k - E[V_k])V_{k+n}]}{E[V_k]^2} \\ R_k &= \frac{V_{k+1} - V_k}{V_{k+1} + V_k} \end{aligned} \quad (3.2)$$

be correlation and reflection coefficients associated with V_k . The covariances of the reflections are

$$a_n = E[R_k R_{k+n}] \sim -(\gamma_{n-1} - 2\gamma_n + \gamma_{n+1})/4. \quad (3.3)$$

To leading order $a_0 = (\gamma_0 - \gamma_1)/2$ is a first order difference and (3.3) in general a second order central difference. Let \mathbf{A} be a lower triangular (semi infinite) Toeplitz matrix whose first column is $[a_0/2, a_1, a_2, \dots]$. Then the non-zero (causal) part of \mathbf{H}_L is the *first column* of the matrix

$$e^{-N\mathbf{A}} \quad (3.4)$$

with $L = N\Delta z$. The pulse shaping filter \mathbf{H}_L can alternatively be expressed as

$$\mathbf{H}_L = \sum_{m=0}^{\infty} p_m \mathbf{q}^{m*} \quad (3.5)$$

where p_m is a discrete Poisson distribution with parameter $a = (a_0/2)N > 0$

$$p_m = \exp(-a)a^m/m!. \quad (3.6)$$

The sequence \mathbf{q} is defined by

$$q_n = \begin{cases} 0 & \text{for } n \leq 0 \\ \frac{-a_n}{a_0/2} \sim \frac{\gamma_{n-1} - 2\gamma_n + \gamma_{n+1}}{\gamma_0 - \gamma_1} & \text{otherwise.} \end{cases}$$

In (3.5) \mathbf{q}^{m*} denotes m-fold convolution and $\mathbf{q}^{0*} \equiv \mathbf{y} = \{y_i\}$ is the sequence with $y_0 = 1$ and $y_i = 0$ for $i \neq 0$. Based on the representation (3.5), we make the following observation. If the sequence $\{\gamma_n\}$ is *convex* for $n \geq 1$, then \mathbf{q} is a *positive* sequence that can be interpreted as a discrete probability distribution and \mathbf{H}_L as the distribution of a random sum. By an application of the central limit theorem, it follows that \mathbf{H}_L is close to the Gaussian distribution for large L . If the sequence $\{\gamma_n\}$ is not convex, there is cancellation in the convolutions \mathbf{q}^{m*} and the pulse shaping filter \mathbf{H}_L does *not* approach the Gaussian bell shape.

The roughness of the medium is crucial in determining the apparent attenuation phenomenon and this property is corrupted by the smoothing effect of the well-log tool. How is this seen in (3.5)? For typical media, for instance a Markovian model medium, the sequence $\{\gamma_k\}$ will be convex. However, replacing V_k by the log \tilde{V}_k entails that the sequence $\gamma = \{\gamma_n\}$ is replaced by $\gamma \star \mathbf{w} \star \bar{\mathbf{w}}$ to leading order; and this sequence is in general *not* convex for $n \geq 1$. Here $\mathbf{w} = \{w_i\}$ is the tool-averaging filter (2.4) and $\bar{\mathbf{w}} = \{w_{-i}\}$. Consequently, the propagating pulse does *not* approach the Gaussian pulse shape. Note also that the crucial parameter a in (3.6) will be much smaller for the medium \tilde{V}_k . Thus, \mathbf{H}_L changes qualitatively due to the tool. We illustrate this in the next section.

4 Simulations

We present results of numerical wave propagation in synthetic media. The simulation will be carried out using a Goupillaud discretization of the medium. That is, a discretization into sections of equal travel times. In the Goupillaud case the O'Doherty-Anstey approximation takes on a similar form to the one presented in (3.4), see Appendix B and [4]. In all the cases we discuss, the source is an *impulse* that probes the medium at the surface $z = 0$. We observe the transmitted pulse at depth $L = 4km$ and plot it relative to its first arrival time. To leading order the transmitted pulse will be \mathbf{H}_L as in (3.5).

We consider four different classes of media

Synthetic media

V_k -The synthetic medium, that is a realization from the model (2.2). The macroscale parameters, \bar{V}_k and e_k , are taken to be *constant*. The pulse shaping depends on the microscale parameters and we use $\epsilon = .03, s = 1.1$ & $l = 2$. These values are estimated from the North Sea log as discussed in Appendix A.

\tilde{V}_k -The synthetic log. This medium is defined by applying the tool model to the synthetic medium as shown in (2.4), see also [7].

Real media

v_k -The ‘real’ medium in the North Sea reservoir. Note that v_k is not explicitly known, only the logged version \tilde{v}_k is available. However, we will use an approximation of v_k that is obtained by deconvolving with respect to the tool model.

\tilde{v}_k -The real well-log obtained from the North Sea reservoir as discussed in Appendix A.

In the sequel we show how replacing a medium by its logged version drastically changes the pulse shaping, the apparent attenuation, due to medium fluctuations. We show this both for the *real* data and the *synthetic* data and also how the O’Doherty-Anstey theory can be used to predict and explain the drastic change.

In Section 4.1 we use several realizations from the model (2.2), several versions of V_k , to illustrate O’Doherty-Anstey pulse shaping in synthetic media that models v_k . This also illustrates the stabilization aspect of the O’Doherty-Anstey theory, that the transformation of the pulse shape to leading order is deterministic. In Section 4.2 we show that the pulse shaping observed in the real well-log, \tilde{v}_k , is very different from the one observed in the medium V_k , but close to the O’Doherty-Anstey prediction of the pulse shaping in the medium \tilde{V}_k . In Section 4.3 we comment on the model for the well-log tool and show that that deconvolving the real log, \tilde{v}_k , with respect to the tool model gives a pulse shaping that is similar to the one seen in the medium V_k ; as it should be if our modeling of the medium and the well-log tool are appropriate. Finally, in Section 4.4 we illustrate briefly how the pulse shaping or blurring of the pulse due to the fine scale medium fluctuations approximately can be removed by deconvolution.

4.1 Pulse shaping and stabilization in synthetic media

First, we illustrate the remarkable stabilization aspect of the O’Doherty-Anstey theory. In *Figure 4.1* we show 30 transmitted pulses corresponding to 30 different realizations of the medium V_k . Despite the fact that the different pulses have traversed different media, different realizations of the model (2.2), their shapes are very similar. This is the stabilization aspect of the O’Doherty-Anstey theory, the transformation of the pulse shape is to leading order deterministic and depends only on media statistics. The travel time on the other hand comprises a small random component. Note that the pulses are plotted relative to their (random) first arrival time. The O’Doherty-Anstey approximation, \mathbf{H}_L , is shown by the stars, and agrees well with the simulations.

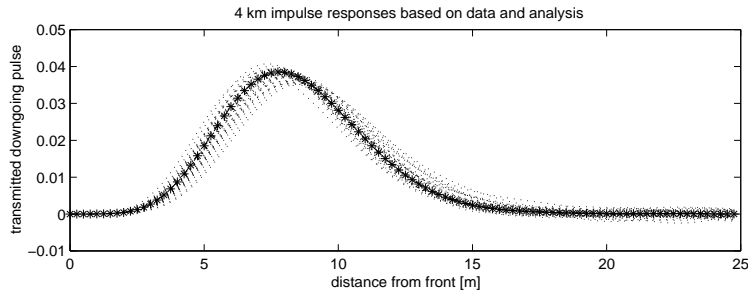


Figure 4.1: The transmitted pulse shape obtained by propagating an impulse through realizations of the synthetic medium, V_k . The 30 dotted lines correspond to different realizations of the medium, all of length $4km$. They agree well with the O’Doherty-Anstey approximation shown by the stars. Note that all pulses are plotted relative to their first arrival time.

4.2 Pulse shaping in the logged medium

Next, we show how the pulse transformation becomes different when we replace the synthetic medium V_k with the synthetic log \tilde{V}_k , but similar to the one in the real log, \tilde{v}_k . The solid line in *Figure 4.2* is the pulse that has propagated through the actual log, \tilde{v}_k , the dashed line is the O’Doherty-Anstey prediction of the transmitted pulse shape for the medium \tilde{V}_k , that is \mathbf{H}_L calculated for this medium. Note the change in scale from the figure above. The medium has been smoothed by the tool and as predicted by the theory of the previous section the transmitted pulse shape is therefore very different; not smooth and bell shaped as above! Note, the excellent agreement between the two pulse shapes in *Figure 4.2*. This is a strong indication that the above modeling of the medium and the measurement tool are appropriate in the context of the wave propagation problem at hand and that the O’Doherty-Anstey approximation well describes the pulse transformation.

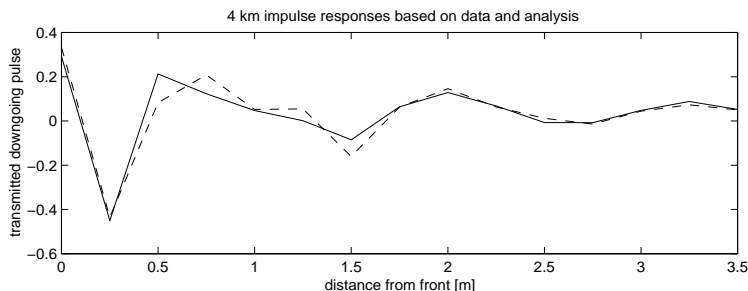


Figure 4.2: The transmitted pulse shapes obtained by propagating an impulse through $4km$ of a medium defined by the real log, \tilde{v}_k , compared with the O’Doherty-Anstey approximation for the synthetic log, \tilde{V}_k , dashed line.

4.3 Pulse shaping in the deconvolved medium

Next, we illustrate how the smoothing of the medium by the tool can be compensated by deconvolution and also motivate our choice for the well-log tool model.

In [7] the tool model corresponding to $\mathbf{w} \propto [1 \ 1 \ 1 \ 1]$ is being used. The length of this filter is defined by the physical length of the tool. We first illustrate deconvolution with respect to these

values for the tool parameters. Based on the tool model (2.4), we design a least-squares deconvolution filter as described in Appendix C. We deconvolve the real log, \tilde{v}_k , with this deconvolution filter. *Figure 4.3* shows the impulse response for the deconvolved medium. The ripples in the transmitted pulse illustrate that the smoothing effect of the tool has not been appropriately compensated. As above we probe the medium with an impulse and plot the transmitted pulse relative to its first arrival time.

In *Figure 4.4* we show the result when we deconvolve the North Sea log using slightly different tool parameters, the parameters $\mathbf{w} \propto [1 \ 1.15 \ 1.3 \ 1.15 \ 1]$. The ripples in the pulse that has propagated through the tool deconvolved real log is now gone and the smoothing effect of the tool has been effectively removed, hence, we use this latter tool model. The dashed line in the figure is the O’Doherty-Anstey approximation of the transmitted pulse corresponding to the synthetic medium V_k . Note that this approximation is remarkable similar to the pulse transmitted through the real deconvolved log, which confirms that the tool effect has been compensated.

We do not pursue the problem of optimal estimation and deconvolution of the measurement tool here. See for instance [18] for a discussion of a Bayesian deconvolution scheme that incorporate a priori information about the stochastic structure of the underlying parameter in addition to a model for the tool.

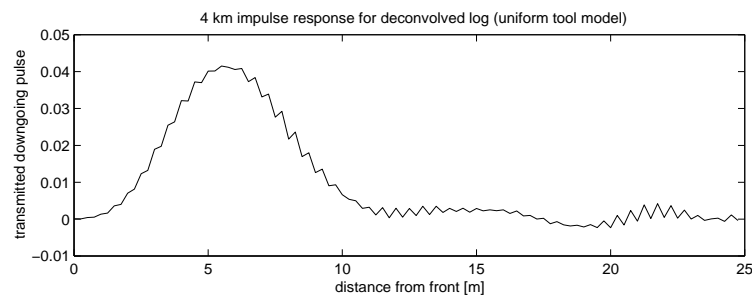


Figure 4.3: The solid line is the transmitted pulse shape obtained by propagating an initially impulsive-like signal through $4km$ of a medium defined by real well-log, \tilde{v}_k , *deconvolved* with respect to the tool. The medium is therefore an approximation of the real medium v_k . However, the ripples in the transmitted pulse show that the smoothing effect of the tool has not been appropriately compensated for.

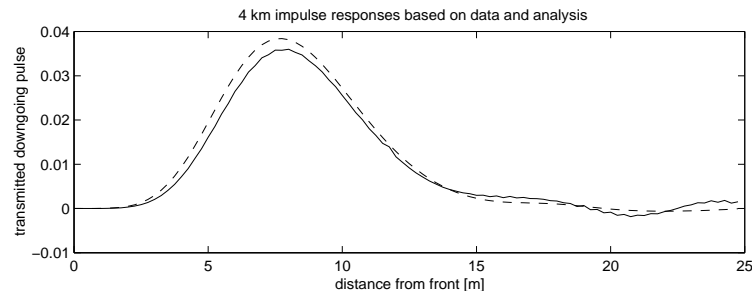


Figure 4.4: The solid line in the figure is defined as the previous figure, except that we used slightly different values for the tool parameters. The pulse shape is smooth and similar to the one in Figure 4.1, thus, the effects of the tool have been compensated for. The dashed line is the O’Doherty-Anstey approximation of the transmitted pulse for the synthetic medium V_k .

Observe that, though there is ‘only one earth’ and one well-log, we modeled it as a random

medium. By modeling the *microscale* fluctuations in the log as a stochastic process and estimating a few parameters in this model, we can accurately analyze and predict the apparent attenuation associated with this one medium, and also similar geological structures. In [17] we show how the pulse-shaping theory can be used to solve the inverse problem. That is, how to estimate the parameters characterizing the microscale fluctuations based on observation of apparent attenuation of the wave. In the next section we illustrate how one can deconvolve with respect to the pulse shaping filter \mathbf{H}_L in order to recover the original wavelet.

4.4 Deconvolution of the pulse shaping

In seismic imaging we wish to identify the macroscopic features of the medium based on observations of the transmitted or reflected signals. These are in general blurred by the fine scale heterogeneities. We show in a very simple context how this blurring effect can be compensated by deconvolution based on the pulse shaping formula (3.1).

In this section we choose the background profile so that the envelope function \bar{V}_k equals 5 between 2000–2100m and 1 elsewhere. Thus, after the first arrival there will be multiples associated with the macroscopic medium variations. The microscale parameters are chosen as above. In [12] it

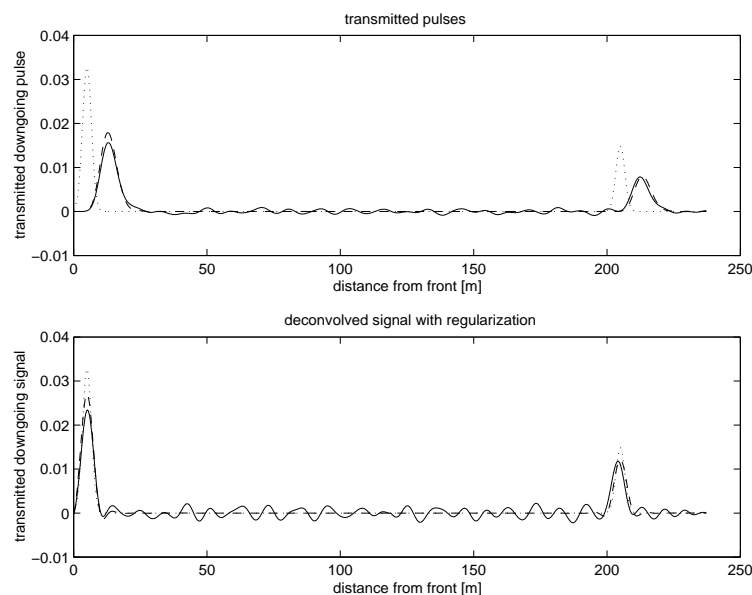


Figure 4.5: The figure illustrates that imbedded features are also being blurred according to the pulse shaping formula and that deconvolution can compensate for the blurring. The solid line in the top plot shows the transmitted signal for a medium with strong macroscopic variations, the dashed line is the O’Doherty-Anstey prediction of the transmitted signal. Note that in this case the probing pulse has the Gaussian bell shape. The dotted line in the figure is the transmitted pulse for the background, without the fine scale structure. We see that the fine scale medium variations has altered the pulse shape. In the bottom plot we deconvolve the transmitted signal with a filter that is approximately the inverse of the pulse shaping effect and get the pulse shape shown by the solid line. This pulse is much closer to the transmitted pulse associated with the background medium, shown with a dotted line. The dashed line is the deconvolved O’Doherty-Anstey approximation.

was shown that the O’Doherty-Anstey theory extends to reflected signals This example illustrates that the approximation indeed accurately predicts the pulse shaping both for the front and for

imbedded features, when we use a realistic model for the fine scale heterogeneities, moreover, that blurring due to fine scale structure can be compensated for by deconvolution.

The transmitted signal is shown by the solid line in *Figure 4.5*, top plot. The dashed line shows the corresponding O’Doherty-Anstey prediction. Note that in this example the source pulse has the Gaussian bell shape. The dotted line corresponds to the transmitted pulse for the background medium, without fluctuations but with the same macroscale envelope and travel times. We see that the fluctuations have modified the pulse shape of the transmitted wave. The effect of the fine scale structure is not negligible.

Next, we attempt to compensate for the blurring effect by convolving the transmitted pulse with a filter which is an approximate inverse of the O’Doherty-Anstey pulse shaping effect as defined by H_L in (3.1). The solid line in the bottom plot of *Figure 4.5* is the deconvolved trace. It agrees much better with the dotted line, the transmitted pulse associated with the background medium. The dashed line is the deconvolved O’Doherty-Anstey prediction. The choice of the deconvolution filter is described in Appendix D. Compensating for the blurring is an ill-posed problem so we introduce a regularization in the deconvolution scheme, which means that some high frequency components of the coherent features of the pulse are lost.

5 Summary and Conclusions

We have examined apparent attenuation in a medium defined by a well-log. A main observation is that apparent attenuation, that is spreading of a pulse due to scattering associated with microscale parameter variation, in the medium defined by the well-log is very different from apparent attenuation in the actual medium. A main result of the study is how a new interpretation of the O’Doherty-Anstey approximation in terms of a random sum can be used to explain this phenomenon. In this interpretation the crucial role of the well-log tool becomes clear, and we show how to compensate for its effect. We also show how to compensate for apparent attenuation by a deconvolution procedure. A main aspect of the study is that we use a *real* well-log, a sonic well-log from the Troll field in the North Sea, to illustrate and confirm the analysis. We obtain excellent agreement between the theoretical predictions derived from the O’Doherty-Anstey approximation and simulations based on this log. In the paper we also introduce a stochastic model for the sonic log and show how to estimate the parameters therein. A significant observation is that the correlation range in this North Sea reservoir is very short, only on the order of one meter and hence on the order of the averaging length of the tool. Another important observation is that for the wave propagation scenario considered, it is sufficient to model the medium in terms of a *two scale* model for an accurate description of multiple scattering effects. We also find that the tool model used in [7] is appropriate for describing the action of the tool.

We believe that the above results are important in the context of generating synthetic seismograms. Moreover, that our modeling and estimation of microscale parameters is of intrinsic interest. These parameters determine not only apparent attenuation due to scattering, but also the statistical structure of the incoherently reflected wave [1] as well as the localization length [16] that determines the penetration depth of the pulse.

6 Acknowledgements

I wish to express my thanks to George Papanicolaou for many helpful discussions. I am grateful to Jim Berryman for carefully reading the manuscript and Eivind Damsleth at Norsk Hydro for providing the well-log data. I acknowledge many useful comments of the reviewers.

References

- [1] M. Ash, W. Kohler, G. C. Papanicolaou, M. Postel, and B. White. Frequency content of randomly scattered signals. *SIAM Review*, 33:519–625, 1991.
- [2] G. E. Backus. Long-wave elastic anisotropy produced by horizontal layering. *J. Geophys. Res.*, 67:4427–4440, 1962.
- [3] R. Burridge, P. Lewicki, and G. C. Papanicolaou. Pulse stabilization in a strongly heterogeneous layered medium. *Wave Motion*, 20:177–195, 1994.
- [4] R. Burridge, G. C. Papanicolaou, and B. White. One dimensional wave propagation in a highly discontinuous medium. *Wave Motion*, 10:19–44, 1988.
- [5] J. Claerbout. *Earth Sounding Analysis. Processing versus inversion*. Blackwell Scientific Publications., 1992.
- [6] J. F. Clouet and J. P. Fouque. Spreading of a pulse travelling in random media. *Annals of Applied Probability*, 4:1083–1097, 1994.
- [7] K. Hsu and R. Burridge. Effects of averaging and sampling on the statistics of reflection coefficients. *Geophysics*, 56:50–58, 1991.
- [8] P. Lewicki. Long time evolution of wavefronts in random media. *SIAM J. Appl. Math.*, 54:907–934, 1994.
- [9] P. Lewicki, R. Burridge, and M. V. de Hoop. Beyond effective medium theory: Pulse stabilization for multimode wave propagation in high contrast layered media. *SIAM Journal on Applied Math.*, 56:256–276, 1996.
- [10] D. Marion, T. Mukerji, and G. Mavko. Scale effects on velocity dispersion: From ray theory to effective medium theories in stratified media. *Geophysics*, 59:1613–1619, 1994.
- [11] R. F. O’Doherty and N. A. Anstey. Reflections on amplitudes. *Geophysical Prospecting*, 19:430–458, 1971.
- [12] G. Papanicolaou and P. Lewicki. Reflection of wavefronts by randomly layered media. *Wave Motion*, 20:245–266, 1994.
- [13] G. C. Papanicolaou and K. Solna. Ray theory for a locally layered random medium. *In preparation*, 1998.
- [14] M. Schoenberger and F. K. Levin. Apparent attenuation due to intrabed multiples. *Geophysics*, 39:278–291, 1974.
- [15] M. Schoenberger and F. K. Levin. Apparent attenuation due to intrabed multiples, II. *Geophysics*, 43:730–737, 1978.
- [16] P. Sheng, B. White, and B. Nair. Lithological correlation and seismic wave localization in the earth’s subsurface. *Inverse Problems*, 5, 1989.
- [17] K. Solna. *Stable spreading of acoustic pulses due to laminated microstructure*. Ph.D. thesis, Stanford University, 1997.
- [18] B. White, P. Sheng, B. Nair, and S. Kerford. Bayesian deconvolution of gamma-ray logs. *Geophysics*, 52:1535–1546, 1987.

A Estimation of well-log parameters

The model for the medium V_k is given in (2.2) and the associated well-log model, \tilde{V}_k , in (2.4). We let the realization of \tilde{V}_k be defined by the sonic log from Block 31/2 of the Troll-field in the North Sea and denote this \tilde{v}_k . This log was kindly provided by Norsk-Hydro. The formation in the Troll-field is assumed to represent a coastal deltaic environment comprising a series of stacked prograding delta lobes resulting in a layered structure dipping about 2-6 degrees. The water depth is about 200m and maximum reservoir depth is about 1700m. We use the observations in the depth range 500 – 1500m. The medium used in the simulation was obtained by first reflecting and then replicating this section.

The three parameters (ϵ, s, l) in (2.2) and (2.3) are the important ones in determining apparent attenuation. We describe their estimation next. We base the estimators on the ‘log reflections’

$$\tilde{r}_k = (\tilde{v}_{k+1} - \tilde{v}_k)/(\tilde{v}_{k+1} + \tilde{v}_k). \quad (\text{A.1})$$

By forming the reflections in (A.1), we mitigate effects of macroscale parameter variations.

The moment estimators are based on comparing the statistics of \tilde{r}_k with the commensurable quantities from the model, that is $\tilde{R}_k = (\tilde{V}_{k+1} - \tilde{V}_k)/(\tilde{V}_{k+1} + \tilde{V}_k)$. We consider respectively the variogram and the histogram. In *Figure A.1* the solid line in the top plot is the variogram of \tilde{r}_k , normalized at maximum lag. The variogram \mathcal{V} of a sequence $\{\tilde{r}_k\}$ is defined by

$$\mathcal{V}(n) = 1/2 \sum_{k=1}^N \frac{(\tilde{r}_k - \tilde{r}_{k+n})^2}{N} \quad (\text{A.2})$$

with $N + n$ being the length of the sequence. The two dotted lines show the statistics when computed based on only the observations in the upper respectively lower halves of the well-log section. The variogram of a realization of \tilde{R}_k is shown by the dashed line. It corresponds to the parameters $\epsilon = .03, s = 1.1$ & $l = 2$. The location of the max value of the variogram in the figure corresponds to the length of the tool, 2 feet. In the bottom plot we show the histograms of the two sequences. Note the long tails of the distribution of \tilde{r}_k that motivates modeling in terms of a log-normal distribution as in (2.2). Before forming the histogram we normalized \tilde{r}_k by an estimate of ϵe_k . This quantity varies only on the macroscale and can be estimated in terms of a moving average of \tilde{r}_k^2 . By simulation we found that the precision of the parameter estimates is approximately 10% for ϵ & s and 20% for l . In [17] we show that the correlation length itself, the integral of the covariance function, is estimated with even higher accuracy.

B Prediction of pulse transformation

We present the O’Doherty-Anstey result that we use in Section 3. Let $V(z)$ be the local speed of sound as a function of depth and assume that the density is constant as above. We model $V(z)$ as a (stationary) stochastic process and denote

$$\frac{E[(V(z) - E[V(z)])V(z+n)]}{E[V(z)]^2} = \gamma(n).$$

If $u_0(t)$ is the pulse shape at the surface $z = 0$, then the shape of the wave pulse when it arrives at depth $z = L$ is [17]

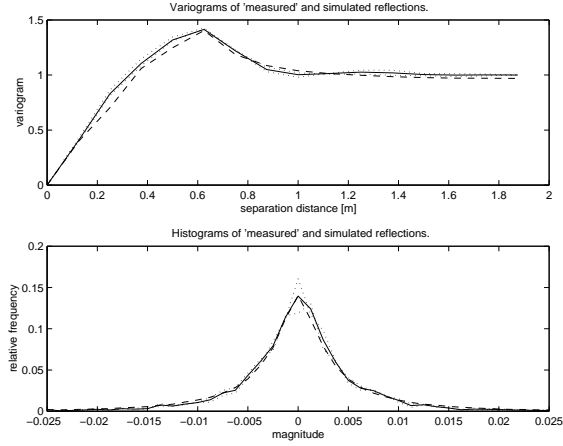


Figure A.1: The figure exhibits some statistics associated with the (nondeconvolved) North Sea sonic log and of a realization of the well-log model \tilde{V}_k . The top plot shows variograms of the reflection coefficients. The solid line corresponds to the entire log section, the dotted lines to data in upper/lower halves and the dashed line to a realization of the model. The correlation structure seems to be stable with respect to depth, and furthermore it matches that of the model. The interpretation of the second plot is similar, however, the histogram rather than the variogram has been computed.

$$u_L(t) \sim u_0 \star \mathcal{H}_L(t) \quad \text{as } \epsilon \downarrow 0,$$

with ϵ being the relative magnitude of the random fluctuations in V . The function \mathcal{H}_L can be characterized by

$$\mathcal{H}_L(t) = \sum_{n=0}^{\infty} p_n q^{n\star}(t).$$

Here $q^{n\star}$ denotes n -fold convolution, $q^0(t) \equiv \delta(t)$ a unit impulse, and p_n is the discrete Poisson distribution with parameter aL where

$$a = -\gamma'(0^+)/4$$

$$q(t/2\bar{V}) = \begin{cases} 0 & \text{for } t \leq 0 \\ -\frac{\gamma''(t)\bar{V}/2}{\gamma'(0^+)} & \text{otherwise} \end{cases}.$$

If $\gamma(t)$ is convex for $t \geq 0$ then \mathcal{H}_L can be characterized as the distribution of a random sum and approaches the Gaussian distribution for large L by the central limit theorem.

Consider next the discrete problem where V is sampled at rate Δz . Let $\gamma_n \equiv \gamma(n\Delta z)$ and use the approximations

$$\begin{aligned} \gamma'(0^+) &\approx (\gamma_1 - \gamma_0)/\Delta z \\ \gamma''(n\Delta z) &\approx (\gamma_{n-1} - 2\gamma_n + \gamma_{n+1})/(\Delta z)^2, \end{aligned} \tag{B.1}$$

then we arrive at the discrete representation (3.5) of \mathcal{H}_L with sampling interval $2\Delta z/\bar{V}$. In [4] the O’Doherty-Anstey approximation is derived for a Goupillaud or equal travel time discretized medium. This approximation can be rewritten in the form (3.5) only that then γ_k represents the correlations of the velocities in the equal travel time sections. However, for a *weakly* heterogeneous medium with small fluctuations this statistics is γ_k to leading order in ϵ when the travel time of a section is $\Delta\tau = \Delta z/\bar{V}$.

C Tool deconvolution

We describe the procedure for deconvolving with respect to the tool. The well-log observations are only weakly correlated and we choose the approximate ‘inverse’ of the tool as the solution to the Wiener-Hopf equations. Let $\mathbf{d} = [d_1, \dots, d_M]$ be the coefficients of the deconvolution filter, they solve $\mathbf{A}\mathbf{d} = \mathbf{b}$. The vector \mathbf{b} is the vector of tool coefficients \mathbf{w} , as in (2.4), padded with zeros. The matrix \mathbf{A} is a symmetric Toeplitz matrix. The i ’th entry of the first row of \mathbf{A} is the i ’th covariance coefficient associated with \mathbf{w} , that is

$$\sum_j w_{i-j} w_j.$$

The dimensions of \mathbf{A} is 20×20 . Then the length of the deconvolution filter is 4 times that of the measurement filter.

D Deconvolution of pulse shaping

We present the deconvolution filter that we use in Section 4 to remove or mitigate the blurring of the pulse caused by the fine scale random fluctuations in the medium parameters. The transmitted pulse at depth L can to leading order be characterized by

$$\mathbf{u}_L \sim \mathbf{u}_e \star \mathbf{H}_L \quad \text{as } \epsilon \downarrow 0$$

with \mathbf{u}_e being the transmitted pulse in the deterministic or effective medium, the medium without the random fluctuations. Thus, to remove the burring effect caused by the random medium fluctuations we deconvolve with respect to \mathbf{H}_L . For the purpose of the illustration we choose the deconvolution filter as the least-squares solution of the system obtained by requiring the convolution of the O’Doherty-Anstey pulse shaping filter, \mathbf{H}_L , with the deconvolution filter to be an impulse. The vector \mathbf{v} of filter coefficients is the least-squares solution of ‘ $\mathbf{A}\mathbf{v} = \mathbf{b}$ ’, with \mathbf{b} being a $5n \times 1$ vector whose coefficients are equal to zero apart from the n ’th entry which is 1. The top $3n \times 2n$ part of \mathbf{A} is a lower triangular Toeplitz matrix whose columns contain the coefficients of the pulse shaping filter. The bottom part, introduced for regularization, much as in [5] page 140, is defined as Δ times the identity matrix. We choose $\Delta = .1$, about the relative strength of the fluctuations in the transmitted trace, and a value for n corresponding to the support of the deconvolution filter being $50m$, roughly twice the spread of the features in the trace.